Topological order-by-disorder in orbitally degenerate dipolar bosons on a zigzag lattice

G. Sun and T. Vekua

Institut für Theoretische Physik, Leibniz Universität Hannover, 30167 Hannover, Germany

(Received 6 February 2014; revised manuscript received 13 August 2014; published 19 September 2014)

Spinor bosons offer a conceptually simple picture of macroscopic quantum behavior of topological order-by-disorder: The paramagnetic state of two-component dipolar bosons in an orbitally degenerate zigzag lattice is unstable against infinitesimal quantum fluctuations of orbitals, λ, towards developing nonlocal hidden order. Adjacent to the topological state a locally correlated exact ground state with spontaneously a quadrupoled lattice constant is realized for the broad parameter regime. The topological order is extremely robust surviving the $\lambda \to \infty$ limit where the ground state evolves into the Majumdar-Ghosh state of a frustrated spin-$\frac{1}{2}$ chain.

DOI: 10.1103/PhysRevB.90.094414 PACS number(s): 03.75.Lm, 03.65.Vf, 05.30.Jp, 75.10.Jm

I. INTRODUCTION

With the realization of the Mott-insulator state of ultracold Bose gas loaded in an optical lattice [1] the groundwork for experimental simulation of magnetism of many-body systems with bosons [2–4] was laid. Since then, with the help of shaking techniques, classical frustrated magnetism has been implemented successfully on triangular lattices [5]. The next target is to simulate quantum magnetism and in particular frustrated quantum spin systems to compensate for the nonexistence of unbiased analytical or numerical methods and observe plausible unconventional ground states à la spin liquids [6,7]. Short-range quantum spin correlations for two-component alkali (contact interacting) Bose gases was exhibited in optical lattices [8]. Using bosonic dipolar atoms (^{52}Cr with strong magnetic dipole moment) nonequilibrium quantum magnetism with long-range exchange physics has been reported in recent experiments [9]. However, a technological breakthrough is needed in reducing temperatures below the spin coherence scales to simulate ground-state equilibrium quantum magnetism in experiments on ultracold gases [10].

Interestingly, lattice bosons can serve as well as excellent analytical simulators of a novel macroscopic quantum effect such as topological order-by-disorder that it is possible to study by simple and at the same time solid arguments.

To show this in this work we study a system of 2-component dipolar bosons in an orbitally degenerate zigzag lattice depicted in Fig. 1. Due to an interplay between the geometric frustration caused by directional character and orbital degeneracy and due to the bosonic nature arbitrary weak quantum fluctuations in orbitals select a topological state from the manifold of extensively degenerate ground states. Adjacent to the topological state, for the broad regime of the system parameters, we also find an exact ground state of the product form with spontaneously broken translational symmetry having a large unit cell made of 4 lattice sites.

Ultracold bosons loaded in the degenerate p bands of optical lattices have attracted considerable theoretical [11,12] and experimental interest [13] due to the possibility of observing chiral superfluids with emerging $p_x \pm ip_y$ order [14].

II. PHYSICAL REALIZATIONS AND EFFECTIVE HAMILTONIAN

Dipolar spinor bosons may be realized using diatomic polar molecules with an electric dipole moment (e.g., potassium-rubidium ^{41}K^{81}Rb [15]) where spin-1/2 degrees of freedom may be encoded in two different total nuclear spin projections of molecules (similar to fermionic case ^{40}K^{81}Rb [16]), resulting in the fact that both the long-range part as well as short-range interactions will be largely spin independent. For fermionic molecules the validity of the assumption of spin independence of interactions was discussed in [17] and similar reasonings hold for bosonic molecules [18].

First we derive the effective Hamiltonian describing the Mott-insulator state of two-component dipolar bosons loaded in doubly degenerate p bands of the zigzag optical lattice where we retain two energetically degenerate orthogonal p_x and p_y orbitals per lattice site. The zigzag lattice may be constructed by the incoherent superposition of a triangular lattice in the xy plane and an additional superlattice [19]. We assume that hopping between neighboring sites is allowed only between the similar orbitals and amplitude of hopping we denote by t as depicted in Fig. 1. Interactions between bosons occupying different sites (when orbitals are spatially separated) are to a good approximation orbital (and as already mentioned spin) independent. For deriving a Hamiltonian describing the Mott phase corresponding to the average occupancy of one boson per lattice site we will consider only interactions between bosons at the same site.

The interaction parameters for two bosons within the same site are given by on-site repulsion within the same orbitals $U_{||}$ and between the orthogonal orbitals $U_{\perp}$,

$$U_{||}(U_{\perp}) = \int d\mathbf{r_1} d\mathbf{r_2}\, p_{\alpha}^2(\mathbf{r_1}) V(\mathbf{r_1}-\mathbf{r_2}) p_{\alpha(\beta\neq\alpha)}^2(\mathbf{r_2}). \quad (1)$$

Here $\alpha,\beta = x,y$, orbital wave functions $p_{x,y}(\mathbf{r})$ are assumed to be centered at one and the same site, and $V(\mathbf{r_1}-\mathbf{r_2})$ is a total interparticle potential including both long-range and contact-repulsive interactions.

Two bosons occupying the same orbital of one site may form a symmetric or antisymmetric state with respect to the orbital index with corresponding energies $U_{||} \pm J_H$ which are split by Hund's exchange due to pair-hopping processes,Â´ as explained in Appendix A,

$$J_H = \int d\mathbf{r_1} d\mathbf{r_2}\, p_x(\mathbf{r_1}) p_y(\mathbf{r_1}) V(\mathbf{r_1}-\mathbf{r_2}) p_x(\mathbf{r_2}) p_y(\mathbf{r_2}). \quad (2)$$

Two bosons occupying orthogonal orbitals of the same site may form a triplet or singlet state in spin variables with corresponding energies $U_{\perp} \pm J_H$ (details are presented

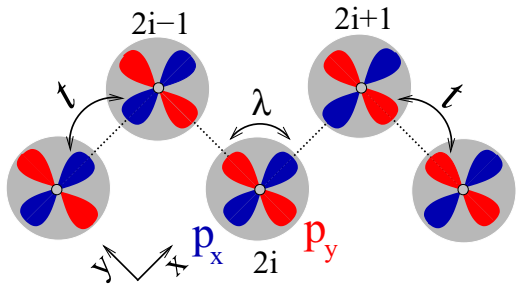

FIG. 1. (Color online) Geometry of the orbitally degenerate zigzag lattice with the intersite hopping t (between similar orbitals) and on-site hopping between the orthogonal orbitals λ.

in Appendix A). In contrast to the fermionic case, Hund's coupling minimizes the total spin of bosons occupying orthogonal orbitals of the same site (even for the case when only contact-repulsive interactions are present). This is due to minimization of interaction energy; by placing two bosons in the antisymmetric $S^T = 0$ spin singlet state the bosonic nature demands that the coordinate wave function be antisymmetric as well; thus it has a node when the distance between bosons vanishes and hence bosons avoid the region where repulsion would be the strongest.

In the strong-coupling limit $U_{||} \pm J_H, U_\perp \pm J_H \gg t$ and with one particle per site the system is in the Mott-insulator regime, and in second-order perturbation theory in t we arrive at the following spin-orbital model (SOM) Hamiltonian (derived explicitly in Appendix A),

$$H = -\sum_i (P_{i,i+1} + 1 - \alpha)\left[1+(-1)^i \sigma_i^z\right]\left[1+(-1)^i \sigma_{i+1}^z\right] + \Delta \sum_i (P_{i,i+1} - 1/2)\left[1 - \sigma_i^z \sigma_{i+1}^z\right], \quad (3)$$

where $P_{i,i+1} = 2\mathbf{S}_i\mathbf{S}_{i+1} + 1/2$ is a permutation operator of spinor components expressed in terms of $\mathbf{S}_i$ spin-$\frac{1}{2}$ operators and σ_i^z is a diagonal Pauli matrix describing the orbital variables, with eigenvalue $+1$ (-1) corresponding to the p_x (p_y) orbital occupied on site i. We have fixed units of $t^2/2\tilde{U} = 1$, with $\tilde{U} = (U_{||}^2 - J_H^2)/U_{||}, \alpha = \tilde{U}(U_\perp - J_H/2)/(U_\perp^2 - J_H^2) \sim U_{||}/U_\perp > 0$, and $\Delta = J_H\tilde{U}/(U_\perp^2 - J_H^2) > 0$. Spin independence of interparticle interactions manifests in explicit SU(2) symmetry of the spin sector.

We note here the crucial role of the long-range part of the interparticle interaction potential in deriving the SOM (3). For a purely contact interaction $V(\mathbf{r}) \sim \delta(\mathbf{r}) \to U_\perp = J_H$, so that in the singlet spin channel two bosons located in the different orbitals of the same site do not experience any scattering. Thus, when only s-wave contact scattering is present (the typical case of alkali atoms), the Mott phase of one boson per lattice well would be unstable due to orbital degeneracy. In the Mott-insulator regime, one can vary both α and Δ in a wide range by changing the lattice depth and a relative ratio of the strengths of the contact and dipolar interactions by modifying the dipole orientation by electric field or by tuning the contact interactions using Feshbach resonances.

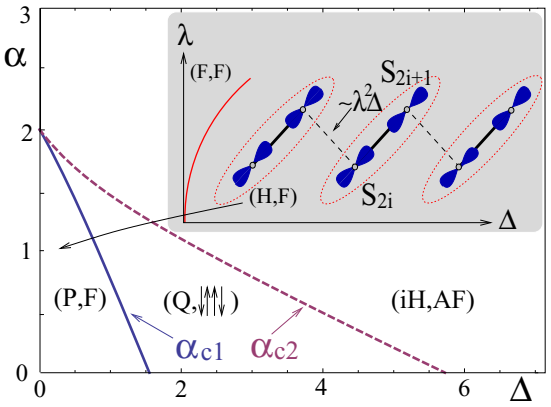

FIG. 2. (Color online) Exact analytical ground state phase diagram of spin-orbital model Eq. (3) obtained in thermodynamic limit. We employ (spin,orbital) notation of different phases. For the ground-state configurations of (Q,↓↑↑↓) and (iH,AF) phases see Fig. 3 and for denotations of phases consult text. Inset shows ground-state orbital configuration of (P,F) phase and the effect in this phase of infinitesimal quantum fluctuations in orbitals λ. Dotted contours encircle 2 sites forming effective spins-1 $\mathbf{T}_i = \mathbf{S}_{2i} + \mathbf{S}_{2i+1}$.

III. GROUND-STATE PHASE DIAGRAM FOR CLASSICAL ORBITALS

Since orbital variables in Eq. (3) are classical it is easy to map out ground-state phases in the product form of spin times orbital part. Depending on values of α and Δ only three different orbital configurations can be realized as ground states for Hamiltonian (3): a period of one ferromagnetic (F) as indicated in the inset of Fig. 2, a period of two antiferromagnetic (AF) as depicted in Fig. 3(b), and a period of four configuration $\cdots p_y p_x p_x p_y \cdots$ (↓↑↑↓) presented in Fig. 3(a).

For $\alpha > 2$ the first line in Eq. (3) selects the AF orbital configuration whereas the Hund coupling Δ induces AF exchange between the spins located on orthogonal orbitals of neighboring sites. In the spin sector one recovers the isotropic Heisenberg antiferromagnet (iH) while in orbitals the doubly degenerate AF configuration remains. Ground-state energy per site in the (iH,AF) state is independent of α and in the thermodynamic limit we can estimate it from an exact solution

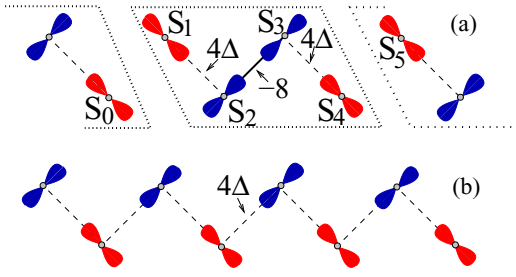

FIG. 3. (Color online) Ground-state orbital configurations in (a) (Q,↓↑↑↓) and (b) (iH,AF) phases. Only occupied orbitals are displayed per site. Dotted contour in (a) encircles cluster of 4 spins decoupled from the rest of the system. Continuous line indicates ferromagnetic Heisenberg exchange between spins at neighboring sites $-8\mathbf{S}_i\mathbf{S}_{i+1}$ and dashed lines indicate AF exchange $4\Delta\mathbf{S}_i\mathbf{S}_{i+1}$.

of the spin-$\frac{1}{2}$ AF Heisenberg chain, $e_0^{iH} = \Delta(1 - 4\ln 2)$. There are no other phases for $\alpha > 2$.

The phase diagram is much more interesting for $0 < \alpha < 2$ as presented in Fig. 2. There, besides the (iH,AF) state we map out 2 additional ground states depending on Δ coupling. For small values of Δ the ground state is twofold degenerate and possesses F orbital order, $\langle\sigma_i^z\rangle = +1(-1)$. Choosing the $\langle\sigma_i^z\rangle = +1$ orbital configuration (this particular orbital order is selected by open boundaries if the chain starts from even number sites; see Fig. 1), two spins on the neighboring sites combine to form an effective spin-1 $\mathbf{T}_i = \mathbf{S}_{2i} + \mathbf{S}_{2i+1}$ in the ground state; however $\mathbf{T}_i$ spins are completely decoupled from each other, thus resulting in an extensively degenerate paramagnetic ground state (P) of spin-1 chain for the spin part of the wave function, with the total degeneracy of the ground state $2 \times 3^{L/2}$ where L is number of sites.

The energy per site for the (P,F) configuration is $e_0^P = 2(\alpha - 2)$ and is independent of Δ. Increasing Δ induces the transition from the (P,F) state to the ground state with the $\downarrow\uparrow\uparrow\downarrow$ configuration of orbitals where bosons can hop only inside spontaneously selected 4-site clusters, as depicted in Fig. 3. For the $\downarrow\uparrow\uparrow\downarrow$ configuration of orbitals, coupling between the spins inside each decoupled cluster of 4 sites (see Fig. 3) is given by $4\Delta\mathbf{S}_1\mathbf{S}_2 - 8\mathbf{S}_2\mathbf{S}_3 + 4\Delta\mathbf{S}_3\mathbf{S}_4 + 4\alpha - 6$ and ground-state energy per site is $e_0^Q = \alpha - 1 - \frac{\Delta}{2} - \sqrt{1 + \Delta + \Delta^2}$. We denote this phase as (Q,$\downarrow\uparrow\uparrow\downarrow$) since spin exchanges have a quadrumerized pattern. Equating two energies $e_0^P = e_0^Q$ we obtain the phase transition line from the (P,F) to the (Q,$\downarrow\uparrow\uparrow\downarrow$) state, $\alpha = \alpha_{c1} = 3 - \frac{\Delta}{2} - \sqrt{1 + \Delta + \Delta^2}$, for any system size that is a multiple of 4.

Further increasing Δ finally system-minimizes its energy for the (iH,AF) state since large Δ, as already mentioned, induces antiferromagnetism for bosons. The phase transition line from the (Q,$\downarrow\uparrow\uparrow\downarrow$) to the (iH,AF) state is obtained by setting $e_0^Q = e_0^{iH}$ and is given in the thermodynamic limit as $\alpha = \alpha_{c2} = 1 + (3 - 4\ln 4)\Delta/2 + \sqrt{1 + \Delta + \Delta^2}$. Different phases of bosons together with phase transition lines are presented in the analytical phase diagram in Fig. 2.

IV. EFFECT OF INFINITESIMAL QUANTUM FLUCTUATIONS IN ORBITALS ON GROUND-STATE PHASES

In reality the zigzag optical lattice is not strictly symmetric in the x-y plane; thus one has to consider the probability of mixing of orbitals,

$$H' = -\sum_i \lambda\sigma_i^x, \tag{4}$$

where λ is the amplitude of the mixing of $p_{x,y}$ orbitals that can be large. First we will study analytically the limit $\lambda \to 0$ where we will observe the topological order-by-disorder phenomenon. Later we address as well another extreme limit analytically $\lambda \gg 1$ and show that topological order survives that limit.

Recently, motivated by simulating transition-metal oxides with partially filled d levels [20–22] containing zigzag chains of spin-$\frac{1}{2}$ ions, a SOM similar to Eq. (3) was introduced for fermions [17] (with an essential difference of the overall sign in front of the Hamiltonian) and it was shown that finite quantum fluctuations in orbitals can stabilize an exotic spin-orbital-liquid phase [23].

The effect of arbitrary weak quantum fluctuation λ on the (P,F) state of bosons is remarkable: the perturbation H' acting as a transverse field in orbitals tries to quantum-disorder orbital order in σ^z variables that is otherwise perfect for $\lambda = 0$, and at the same time, most importantly, it introduces exchange interactions between the decoupled neighboring spins of the (P,F) state,

$$\lim_{\lambda\to 0} H_S = -\sum_i 8\mathbf{S}_{2i}\mathbf{S}_{2i+1} + \chi_\lambda \sum_i \mathbf{S}_{2i+1}\mathbf{S}_{2i+2}, \tag{5}$$

where $\chi_\lambda \simeq \lambda^2\Delta/2(1-\Delta)^2 - O(\lambda^4)$. In particular, in the limit $\lambda \to 0$ the two neighboring spins $\mathbf{S}_{2i}$ and $\mathbf{S}_{2i+1}$ are coupled ferromagnetically with each other with the strength that is infinitely stronger than antiferromagnetic coupling between $\mathbf{S}_{2i+1}$ and $\mathbf{S}_{2i+2}$. Hence for $\lambda \to 0$ the ground-state wave function of the spin part of Eq. (5) coincides with the ground state of the spin-1 chain [24] and a topological (H,F) state is established with nonlocal string order [25]. One can determine the boundary of the (H,F) state $\Delta_F \sim \lambda^2$ for $\Delta \to 0$. For $\Delta < \Delta_F$ the fully polarized (F,F) state is selected for the ground state, and for $\Delta > \Delta_F$ the (H,F) state is stabilized. Thus, for $\Delta > 0$ infinitesimal quantum fluctuations $\lambda \to 0$ select from the extensively degenerate ground-state manifold (P,F) a doubly degenerate state for periodic boundary conditions (degeneracy is due to orbital F order) and a fourfold-degenerate state for open boundary conditions. As already mentioned open boundaries remove orbital degeneracy and hence the residual fourfold degeneracy is purely due to the edge spins of the topological state.

Extensive ground-state degeneracy at the classical level [similar to the (P,F) phase for $\lambda = 0$] is a characteristic property of many frustrated spin systems [26]. If degeneracy can be lifted either by thermal [27,28] or by quantum fluctuations [29,30] and as a result magnetic order develops, such behavior is referred to as order-by-disorder. No unambiguous experimental confirmation of order-by-disorder has been reported in condensed matter magnetic systems, though there are suggestions to simulate it in experiments on ultracold spinor Bose gases [31,32]. Order by quantum disorder in orbitally frustrated electron systems was predicted in two-dimensional square lattices [33]. Here we encounter the emergence of topological order by quantum disorder in orbitally frustrated one-dimensional dipolar spinor bosons.

Other phases depicted in Fig. 2 are stable with respect to infinitesimal quantum fluctuations in orbitals λ. In particular in the (Q,$\downarrow\uparrow\uparrow\downarrow$) state the end spins of two adjacent decoupled (for $\lambda = 0$) 4-spin clusters will get coupled due to λ by AF exchange; i.e., the cluster on Fig. 3 will be coupled to its neighbors by terms $\sim \Delta\lambda^2(\mathbf{S}_0\mathbf{S}_1 + \mathbf{S}_4\mathbf{S}_5)$.

V. GROUND-STATE PHASES FOR STRONG QUANTUM FLUCTUATIONS IN ORBITALS

Apart of the above determined exotic ground states for $\lambda \to 0$ and the discovered effect of topological order-by-disorder, the bosonic problem studied here turns out to be

relevant for realistic condensed matter systems. To show this we address another limit, $\lambda \gg 1$.

We may then decompose $H + H' = H_0 + V$, where $H_0 = -\lambda \sum_i \sigma_i^x + 2(1-\Delta)\sum_i \mathbf{S}_i\mathbf{S}_{i+1}$, and V may be treated as a perturbation. To the lowest order in $1/\lambda$ the system becomes equivalent to a spin-$\frac{1}{2}$ j_1-j_2 chain,

$$\lim_{\lambda\to\infty} H_S = \sum_i [j_1 \mathbf{S}_i\mathbf{S}_{i+1} + j_2 \mathbf{S}_i\mathbf{S}_{i+2}], \tag{6}$$

with $j_1 = 2(\Delta-1) + (4-\Delta+\Delta^2)/2\lambda$ and $j_2 = \lambda^{-1}$. Higher order terms $\sim 1/\lambda^2$ involve biquadratic terms in spin operators as well as bilinear interactions beyond second nearest neighbor and present irrelevant deviation from the j_1-j_2 chain similarly to the fermionic case [17]. Note that the original microscopic model at $\alpha = 1$ for bosons differs just by an overall sign from the corresponding fermionic expression [17]; however it is not exactly the case for the effective spin models in large λ. From the known ground-state phase diagram of the spin-$\frac{1}{2}$ j_1-j_2 zigzag chain with $j_2 > 0$ we map out ground-state phases for our bosonic system in the strong λ limit. For $\Delta > 1 + 1/\lambda$ the system can be mapped on the j_1-j_2 zigzag chain with $j_1 > 4j_2$ with the gapless ground state of the isotropic Heisenberg chain. Orbital correlations are paramagnetic. We denote this phase by (iH,P). For $1 - 1/\lambda < \Delta < 1 + 1/\lambda$ the spin sector can be mapped onto the SU(2) symmetric frustrated antiferromagnetic spin-$\frac{1}{2}$ chain with $0 < j_1 < 4j_2$ with dimerized ground state. The representative state in this phase is realized for $j_1 = 2j_2$ and is called the Majumdar-Ghosh state [34] that is made of the direct product of singlets involving the nearest spins. Because of the linear coupling between spin dimerization and orbitals present in Hamiltonian Eq. (3), $\sum_i (\mathbf{S}_i\mathbf{S}_{i+1} - \mathbf{S}_i\mathbf{S}_{i-1})\sigma_i^z$, dimerization order in spin variables $\langle \mathbf{S}_i\mathbf{S}_{i+1} - \mathbf{S}_i\mathbf{S}_{i-1}\rangle \neq 0$ is felt as a uniform magnetic field in orbital variables. Hence the occurrence of the dimerization pattern in spin variables will be accompanied by developing ferromagnetic correlations in orbital variables leading to a dimer-ferro phase (D,F).

For $1 - 3/\lambda < \Delta < 1 - 1/\lambda$ the system can be mapped on the SU(2) symmetric frustrated ferromagnetic spin-$\frac{1}{2}$ chain with $0 > j_1 > -4j_2$. Numerical study of the ground state of the frustrated ferromagnetic chain based on the infinite-size algorithm suggests that the nearest bonds are characterized by ferro correlations with alternating strengths, and the phase was dubbed the Haldane dimer [35].

Finally in spin variables we obtain a fully polarized ferromagnetic state for $\Delta < 1 - 3/\lambda$, whereas orbital variables become paramagnetic again (F,P).

In the next section we present the numerical ground-state phase diagram for all values of λ which shows that our bosonic model interpolates smoothly between the Majumdar-Ghosh state of the (D,F) phase realized for $\lambda \gg 1$ and an exact Haldane state of an effective spin-1 chain realized for $\lambda \to 0$.

VI. NUMERICAL SIMULATIONS

In the remaining we support our analytical findings numerically by simulating directly the full microsopic SOM including quantum fluctuations of orbitals, $H + H'$. To address large systems we use the density matrix renormalization group method [36] that is implemented best with open boundary conditions. The results of the numerical simulations of the SOM presented below are for open system with $L = 96$ sites and we compare them with the analogous results for the Haldane chain on $L = 48$ sites to show that for $\lambda \to 0$ the ground-state configuration of the spin part of the SOM reproduces identically the topologically nontrivial ground state of the antiferromagnetic SU(2) symmetric spin-1 chain. With increasing λ the Haldane state for periodic boundary conditions adiabatically evolves into the dimerized state of the spin-$\frac{1}{2}$ chain.

A. Small λ case

First we present numerical results of short-range ground-state correlation functions between the neighboring spins as a function of λ in the (H,F) state in Fig. 4 for $\lambda \ll 1$. As expected from analytical analyses one can observe in Fig. 4 that in the limit $\lambda \to 0$, $\langle \mathbf{S}_{2i}\mathbf{S}_{2i+1}\rangle = \langle \mathbf{S}_{2i+2}\mathbf{S}_{2i+3}\rangle = 1/4$ and $\langle \mathbf{S}_{2i+1}\mathbf{S}_{2i+2}\rangle = \langle \mathbf{S}_{2i}\mathbf{S}_{2i+2}\rangle = \langle \mathbf{S}_{2i+1}\mathbf{S}_{2i+3}\rangle = \langle \mathbf{S}_{2i}\mathbf{S}_{2i+3}\rangle \simeq -0.35$ so that $\langle \mathbf{T}_i\mathbf{T}_{i+1}\rangle = \langle (\mathbf{S}_{2i} + \mathbf{S}_{2i+1})(\mathbf{S}_{2i+2} + \mathbf{S}_{2i+3})\rangle \simeq -1.4 \simeq e_0(S=1)$, where $e_0(S=1)$ is the well known value of the ground-state energy per site of the spin-1 chain [36] (in the units of exchange) that is equal to the ground-state correlation function of two neighboring spins of the Haldane chain.

The Néel correlation function $(-1)^{j+i}\langle T_j^z T_{j+i}^z\rangle$ and string correlation function $-\langle T_j^z e^{i\pi\sum_{k=j+1}^{j+i-1} T_k^z} T_{j+i}^z\rangle$ are presented in Fig. 5(a) for both the SOM on L sites ($L = 96$) and Haldane chain on $L/2$ sites. As one can see the coincidence between the results for the Haldane chain and SOM in the (H,F) state for small λ is excellent.

Finally, the magnetization profile of the SOM $\langle \mathbf{S}_{2i} + \mathbf{S}_{2i+1}\rangle$ in one of the ground states of the Kennedy-Tasaki triplet [37] with total $S^z = 1$ is presented in Fig. 5(b). On the same plot we superimpose this profile with the corresponding profile of the Haldane chain [36] and again observe the perfect matching between the two.

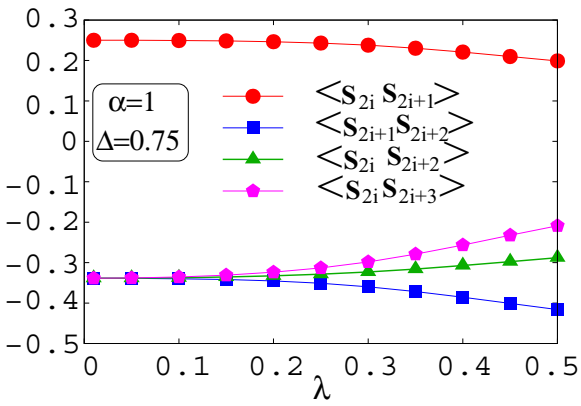

FIG. 4. (Color online) Bulk short-range spin correlation function's dependence on λ in (H,F) phase. Due to extensive degeneracy of ground states in (P,F) phase, numerically we cannot approach arbitrarily close to $\lambda = 0$, but the tendency is evident. Symmetry with respect to translations on 2 sites of (H,F) state imposes $\langle \mathbf{S}_{2i}\mathbf{S}_{2i+1}\rangle = \langle \mathbf{S}_{2i+2}\mathbf{S}_{2i+3}\rangle$ and $\langle \mathbf{S}_{2i}\mathbf{S}_{2i+2}\rangle = \langle \mathbf{S}_{2i+1}\mathbf{S}_{2i+3}\rangle$.

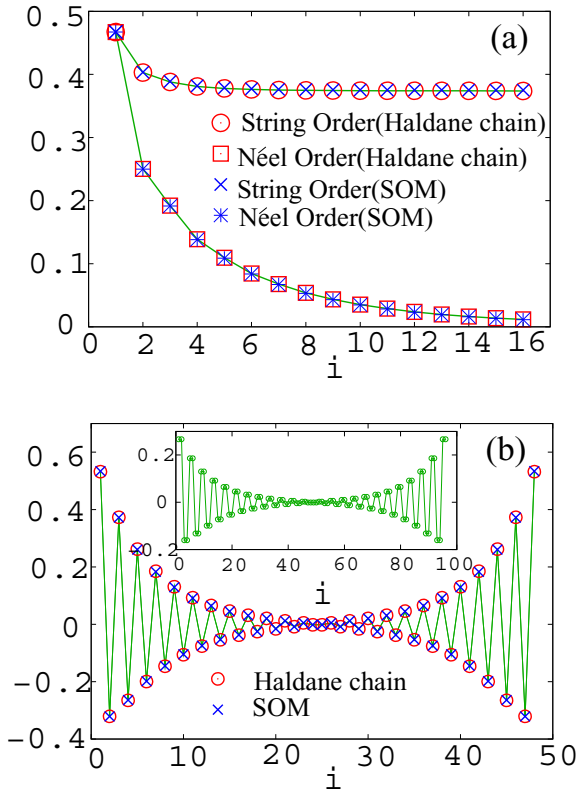

FIG. 5. (Color online) (a) Blue symbols: Bulk Néel order and string order of spin-orbital model (SOM) in (H,F) phase for $\lambda \to 0$ (here $\lambda = 0.1$, $\alpha = 1$, and $\Delta = 0.1$). Red symbols: Corresponding order parameters of spin-1 Haldane chain. (b) Magnetization profile in $S^z = 1$ Kennedy-Tasaki ground state of spin-1 Haldane chain on $L = 48$ sites (red symbols) is nearly identical to magnetization profile of $\langle T_i^z \rangle = \langle S_{2i}^z + S_{2i+1}^z \rangle$ of SOM on $L = 96$ sites (blue symbols) in (H,F) phase for $\lambda \to 0$ (here $\lambda = 0.1$, $\alpha = 1$, and $\Delta = 0.1$). Inset (green circles) shows site-resolved magnetization profile of SOM $\langle S_{2i}^z \rangle \simeq \langle S_{2i+1}^z \rangle \simeq \langle T_i^z \rangle / 2$.

B. General λ case

We present the numerical ground-state phase diagram in the full parameter space of Δ versus λ in Fig. 6.

The simplest task is to determine the boundary of the fully polarized ferromagnetic state since the total spin of the ground state jumps from the maximal $S^T = L/2$ value to $S^T = 0$. Inside the fully polarized region for the orbital sector we obtain an exactly solvable quantum Ising model in transverse magnetic field. Hence there is an Ising phase transition with increasing λ between the (F,F) and (F,P) states at $\lambda = 2 - \alpha + \Delta/2$. Ising phase transitions are usually captured numerically with studying fidelity susceptibility. For a generic Hamiltonian, with a phase transition driven by the changing strength of coupling constant λ, the fidelity susceptibility (FS) χ with respect to the "perturbation" λ is defined as [38,39]

$$\chi = \lim_{\delta\lambda \to 0} \frac{1 - |\langle \psi_0(\lambda) | \psi_0(\lambda + \delta\lambda) \rangle|^2}{\delta\lambda^2}, \tag{7}$$

where $|\psi_0(\lambda)\rangle$ is the ground-state vector for given λ.

We have studied numerically fidelity susceptibility inside the fully polarized phase and obtained the phase transition line between (F,F) and (F,P) phases that matches accurately the analytical result.

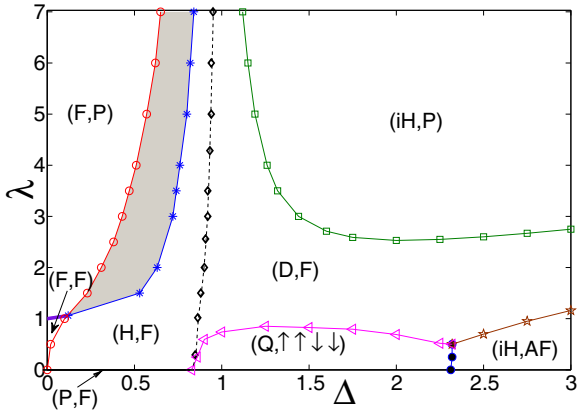

FIG. 6. (Color online) Effect of λ on ground-state phases presented in Fig. 2 for $\alpha = 1$. Dashed line between (H,F) and (D,F) phases represents a boundary phase transition, where edge spins at the end of the open chain disappear in (D,F) phase. All second-order phase transition lines are obtained with extrapolation procedure from finite system size data to infinite size.

Similarly, between two gapped phases (Q,↓↑↑↓) and (D,F) due to symmetry considerations we expect the Ising phase transition. Scaling of the height of the peak of fidelity susceptibility with system size depicted in Fig. 7 confirms our expectations.

Based on the behavior of order parameters, ground state, and low-energy excited states the phase transition from the (iH,AF) to (D,F) phase seems a smooth second-order transition. On general grounds we expect a Gaussian phase transition, respecting the SU(2) symmetry of the spin sector, driven by a marginal operator, being marginally irrelevant in the gapless (iH,AF) phase and becoming marginally relevant in the gapped (D,F) phase. Hence scaling of the fidelity susceptibility per site should be sublinear. Surprisingly to us, scaling of the fidelity susceptibility peak per site with system size in the vicinity of the phase transition from the (iH,AF) to

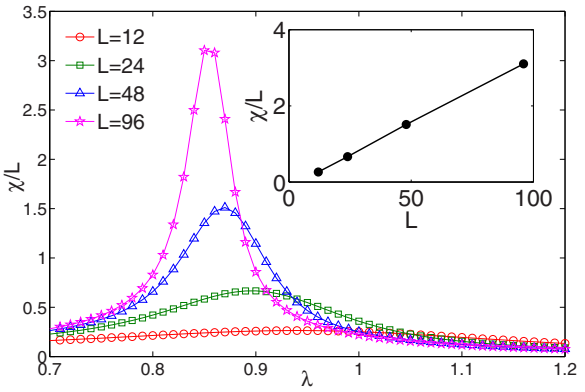

FIG. 7. (Color online) FS with respect to λ per site for $\Delta = 1.5$, $\alpha = 1$. Linear scaling of fidelity susceptibility peak per site with system size confirms Ising nature of quantum phase transition from the (Q,↓↑↑↓) to (D,F) state.

(D,F) state is also linear as for the Ising case. However, the transition between the gapless (iH,AF) phase and gapped (D,F) phase cannot be of Ising nature. We interpret the linear scaling in the following way: since FS does not capture transition from the (D,F) to (iH,P) state (that is witnessed by singlet-triplet level crossing in the first excited states) from the FS point of view transition from (iH,AF) to (D,F) is similar to the transition from the (iH,AF) directly to the (iH,P) state that would be of Ising nature. Not only the height of the FS peak per site scales linearly with system size but also the position of the peak scales perfectly linearly with the inverse system size.

For open boundary conditions, (D,F) has a unique ground state, whereas (H,F) has a fourfold-degenerate ground state due to the edge spins. Hence these two phases cannot be smoothly connected for the case of open boundary conditions. For periodic boundary conditions the Haldane state is smoothly connected with the (D,F) state and the ground-state degeneracy is twofold. Pure spin models which interpolate smoothly between the Haldane state and dimerized state have been studied in [40–42].

For values of $\lambda > 2$ the topology of the ground-state phase diagram is similar to the fermionic case obtained in the strong λ case [17], though with reversed sequence of phases with increasing Δ ($\Delta_{\text{Boson}} \to 1/\Delta_{\text{Fermion}}$), and an identical approach to that reported in [17] was performed to determine these phases and boundaries between them. In particular dimerization order vanished at the boundary of the shaded region (indicated by star symbols in Fig. 6) and then reappears again inside the shaded region. However dimer order is very small adjacent to the (F,P) state where we cannot exclude occurrence of other additional phases, though the ground state is a global singlet until reaching the (F,P) phase.

According to our numerical data, in particular due to very fast growth of the height of peak of fidelity susceptibility, we interpret the phase transition between (Q,↓↑↑↓) and (iH,AF) phases as first order.

VII. CONCLUSIONS

In conclusion, dipolar spinor bosons in orbitally degenerate zigzag lattices develop topological order in extensively degenerate paramagnetic states due to arbitrary weak quantum fluctuations of orbitals. This is a direct consequence of the interplay between the orbital frustration and the bosonic nature. Adjacent to the topological state the exact ground state is obtained with spontaneously quadrupoled unit cells for the broad parameter regime of Hund's coupling and the ratio between on-site and long-range interactions. Moreover, by changing the strength of quantum fluctuations of orbitals our model interpolates between the exact ground state of the Haldane chain (realized for $\lambda \ll 1$) and the Majumdar-Ghosh state of the spin-$\frac{1}{2}$ chain (realized for $\lambda \gg 1$).

In our theoretical work we have not addressed effects of interactions beyond the single site. Due to symmetry of the microscopic bosonic model and restricting with quadratic terms in hoppings, the form of the effective spin-orbit Hamiltonian will not change by including interactions beyond on-site; however expressions of constants will be modified. Dipolar interactions fall off rapidly with the distance; hence gapped phases such as the topological Haldane phase as well as (Q,↓↑↑↓) and (D,F) will be robust with inclusion of dipolar interactions beyond the on-site contribution, though their boundaries will be modified. We have so far ignored the effect of population of s orbitals. In experimental realization efficiency of populating p orbitals will clearly be less than 100%; moreover, due to interorbital collisions the lifetime in p orbitals will be limited. Neither have we addressed the effects of finite temperature, whereas in experiments on multicomponent ultracold gases the biggest challenge is to reduce the temperature below the spin coherence scale set by superexchange interaction. All these effects need to be addressed before experimental realization of the obtained results in ultracold gases.

ACKNOWLEDGMENTS

We thank G. Jackeli for interesting us in spin-orbital models. This work has been supported by QUEST (Center for Quantum Engineering and Space-Time Research) and DFG Research Training Group (Graduiertenkolleg) 1729.

APPENDIX A: MICROSCOPIC DERIVATION OF EFFECTIVE MODEL

In this appendix we provide details of derivation of our spin-orbital model Eq. (1), generalizing calculation for orbitally degenerate electrons [43] to the bosonic case. First we decompose the bosonic field operator into a Wannier function basis centered at zigzag lattice sites $\mathbf{r}_j$,

$$\psi_s(\mathbf{r}) = \sum_j [\omega_1(\mathbf{r}-\mathbf{r}_j) b_{1\,j,s} + \omega_2(\mathbf{r}-\mathbf{r}_j) b_{2\,j,s}]. \tag{A1}$$

For a deep lattice the Wannier functions can be approximated as $p_{x,y}$ orbitals of harmonic oscillator $\omega_2 \to p_x$ and $\omega_1 \to p_y$; however true Wannier functions are less localized and most importantly at tails they oscillate to provide orthogonality between the functions centered at different sites.

Above we have introduced the bosonic annihilation operator $b_{a\,j,s}$ at site $\mathbf{r}_j$, where the orbital index $a = 1$ (2) refers to the p_y (p_x) orbital and index $s = \uparrow, \downarrow$ refers to the spin.

Two-component Bose gas in a periodic (laser induced) lattice potential $V(\mathbf{r})$ is described by a generic Hamiltonian,

$$H_B = \sum_s \int \psi_s^\dagger(\mathbf{r}) \left[-\frac{\hbar^2}{2m}\nabla^2 + V(\mathbf{r}) \right] \psi_s(\mathbf{r}) d\mathbf{r} + \sum_{s,s'} \int \psi_s^\dagger(\mathbf{r}_1) \psi_{s'}^\dagger(\mathbf{r}_2) \frac{V(\mathbf{r}_1 - \mathbf{r}_2)}{2} \psi_{s'}(\mathbf{r}_2) \psi_s(\mathbf{r}_1) d\mathbf{r}_1 d\mathbf{r}_2. \tag{A2}$$

Substituting decomposition (A1) into Hamiltonian (A2) after standard truncations we arrive at the tight-binding type model $H_{\text{TB}} = H_k + H_{\text{int}}$, where

$$H_k = -\frac{t}{2} \sum_{i,a,s} [1 + (-1)^{i+a}][b_{a\,i,s}^\dagger b_{a\,i+1,s} + b_{a\,i+1,s}^\dagger b_{a\,i,s}]$$

accounts for single-particle processes, describing intersite tunneling between similar orbitals in zigzag patterns (as

depicted in Fig. 1), and

$$H_{\rm int} = \frac{U_{||}}{2}\sum_{i,a,s,s'} b^\dagger_{a\,i,s} b^\dagger_{a\,i,s'} b_{a\,i,s'} b_{a\,i,s} + U_\perp \sum_{i,s,s'} b^\dagger_{1\,i,s} b_{1\,i,s} b^\dagger_{2\,i,s'} b_{2\,i,s'} + 2J_H \sum_i \left[\mathbf{S}_{1\,i}\mathbf{S}_{2\,i} + \frac{n_{1\,i}n_{2\,i}}{4}\right] + J_H \sum_i [b^\dagger_{1\,i,\uparrow} b^\dagger_{1\,i,\downarrow} b_{2\,i,\downarrow} b_{2\,i,\uparrow} + \text{H.c.}] + \frac{J_H}{2}\sum_{i,s} [b^\dagger_{1\,i,s} b^\dagger_{1\,i,s} b_{2\,i,s} b_{2\,i,s} + \text{H.c.}] \quad \text{(A3)}$$

corresponds to two-particle interactions. Interaction parameters are given in Eqs. (1) and (2).

This form of the interaction part is particularly convenient for deriving an effective spin-orbital model. The first two lines in Eq. (A3) describe the usual density-density interactions for the case of two bosons occupying the same orbital (first line) and different orbitals (second line) correspondingly; the third line describes the Hund exchange when two bosons occupy orthogonal orbitals and the last two lines are called pair hopping processes of two bosons from one orbital to another. Due to considerations of symmetry [43] terms containing $\int d\mathbf{r_1} d\mathbf{r_2} p_{\beta\neq\alpha}(\mathbf{r_1}) p_\alpha(\mathbf{r_1}) V(\mathbf{r_1}-\mathbf{r_2}) p_\alpha(\mathbf{r_2}) p_\alpha(\mathbf{r_2})$ are neglected.

Now we assume that interactions dominate over kinetic energy and concentrate on the filling corresponding to one boson per site. First we put hopping $t = 0$ and diagonalize the interaction part Eq. (A3). The lowest energy state is when each site is occupied by one boson (singly occupied sites). For $t = 0$ this state is degenerate extensively 4^L due to orbital and spin degeneracy. Considering hopping t as a perturbation we want to project the effective Hamiltonian on the states with a single boson per site. For this we have to consider virtual states that are obtained from singly occupied states after the hopping of one boson from one site to its neighboring site (hence one site is empty and a neighboring site is occupied by two bosons). When two bosons are located on one and the same orbital of the same site ($|p_x,p_x\rangle$ and $|p_y,p_y\rangle$) these state are not eigenstates of $H_{\rm int}$ due to pair hopping processes. Rather symmetric and antisymmetric orbital combinations are eigenstates $|\pm\rangle = |p_x,p_x\rangle \pm |p_y,p_y\rangle$, $H_{\rm int}|\pm\rangle = (U_{||} \pm J_H)|\pm\rangle$. Naturally both states $|\pm\rangle$ are invariant with respect to exchanging the coordinates of two bosons and hence the spin part of the wave function is as well the symmetric triplet state

$$H_{\rm eff} \to -P_{||}\frac{H_k|+\rangle\langle+|H_k}{\Delta E = U_{||}+J_H}P_{||} - P_{||}\frac{H_k|-\rangle\langle-|H_k}{\Delta E = U_{||}-J_H}P_{||},$$

where $P_{||}$ is a projector on the ground-state manifold of $H_{\rm int}$ having one boson per site with two neighboring bosons occupying similar orbitals. Analogically we have to consider the case of projectors on the ground-state manifold of $H_{\rm int}$ having one boson per site with two neighboring bosons occupying different orbitals $P_\perp$. In the latter case one has to distinguish between symmetric and antisymmetric configurations in spin space, equivalently in coordinate space due to the bosonic symmetrization principle, $H_{\rm int}(|p_x,p_y\rangle \pm |p_y,p_x\rangle) = (U_\perp \pm J_H)(|p_x,p_y\rangle \pm |p_y,p_x\rangle)$. Note that due to the third line in Eq. (A3) the eigenstates $H_{\rm int}$ where two bosons occupy orthogonal orbitals of the same site are $|p_x,p_y\rangle \pm |p_y,p_x\rangle$.

Putting all contributions together in second order of perturbation theory in hopping t we obtain the effective Hamiltonian of the form $\sum_i H_{i,i+1}$, where $H_{i,i+1}$ is the two-site Hamiltonian:

$$H_{i,i+1} = -\frac{t^2}{\tilde{U}}P_{i,i+1}(S^T{=}1)\left[1+(-1)^i\sigma^z_i\right]\left[1+(-1)^i\sigma^z_{i+1}\right] - \frac{t^2}{2(U_\perp - J_H)}P_{i,i+1}(S^T{=}0)\left(1-\sigma^z_i\sigma^z_{i+1}\right) - \frac{t^2}{2(U_\perp + J_H)}P_{i,i+1}(S^T{=}1)\left(1-\sigma^z_i\sigma^z_{i+1}\right). \quad \text{(A4)}$$

Above we have introduced singlet and triplet projector operators $P_{i,i+1}(S^T{=}0) = -\mathbf{S}_i\mathbf{S}_{i+1} + 1/4$, and $P_{i,i+1}(S^T{=}1) = \mathbf{S}_i\mathbf{S}_{i+1} + 3/4$, which project onto two-boson states on sites i and $i+1$ with, respectively, total spin $S^T = 0$ and $S^T = 1$, where

$$\mathbf{S}_i = \sum_a \mathbf{S}_{a\,i} = \frac{1}{2}\sum_{a,s,s'} b^\dagger_{a\,i,s}\boldsymbol{\sigma}_{s,s'} b_{a\,i,s'}$$

with $\boldsymbol{\sigma}$ denoting Pauli matrices.

The Hamiltonian $\sum_i H_{i,i+1}$, where $H_{i,i+1}$ is given in Eq. (A4), is equivalent to Hamiltonian Eq. (1). Quantum fluctuation of orbitals described in Eq. (2) is caused by a finite on-site tunneling between p_x and p_y orbitals due to finite lattice asymmetry (mixing p_x and p_y orbitals), $-\lambda\sum_{i,s}(b^\dagger_{1\,i,s}b_{2\,i,s} + b^\dagger_{2\,i,s}b_{1\,i,s})$.

APPENDIX B: LATTICE ON-SITE ENERGIES OF DIPOLAR BOSONS IN *p*-BANDS

Here we discuss on-site interaction energies of dipolar bosons in p-bands of zigzag optical lattice that may be realized by incoherent superposition of triangular lattice and an additional superlattice [19]. We will estimate system parameters for the case of a quasi-2D square lattice $V(\mathbf{r}) = V_0(\sin^2\pi x/a + \sin^2\pi y/a + \frac{V_0^z}{V_0}\sin^2\pi z/a)$ and neglect modification due to the additional superlattice. To simplify further estimation we will use the harmonic approximation and take $V_0^z/V_0 = 2$ and $V_0 = 25E_R$ (the optical lattice should be deep enough to neglect the tunneling of molecules in s orbitals), where $E_R = \frac{\hbar^2\pi^2}{2ma^2}$ is recoil energy, m mass of molecule, and $a = 0.5\ \mu$m (typical lattice constant for optical lattices). We note that harmonic approximation overestimates interaction energies and may even (for the case of average occupation of particles per site greater than 1) miss quantitative features [44]; however it may serve as a rough estimate of interaction energies involved in the problem.

We divide the on-site interaction energies into a contact part and dipolar part, $U_{||(\perp)} = U^c_{||(\perp)} + U^d_{||(\perp)}$. In the case of disoriented dipoles the dominant on-site contribution comes from the contact s-wave scattering: for bosons occupying the same orbital $U^c_{||} = \frac{4\pi a_s\hbar^2}{m}\int d\mathbf{r}\, p^4_\alpha(\mathbf{r}) \sim 0.5E_R$, for s-wave scattering length $a_S \sim 100a_0$, with a_0 being the Bohr radius. On-site interaction for bosons occupying orthogonal orbitals is

$U^c_\perp = \frac{4\pi a_s \hbar^2}{m} \int d\mathbf{r}\, p_x^2(\mathbf{r}) p_y^2(\mathbf{r}) = U^c_{||}/3$, the ratio $U^c_\perp/U^c_{||} = 1/3$ being independent of V_0^z/V_0 in the harmonic approximation. To estimate the dipolar contribution in on-site energies we Fourier-transform the dipolar potential and use a similar approximation as discussed for the dipolar Bose gas in the spherical trap [45] as well as in the presence of an optical lattice [46]. For molecules with strong dipolar moment (of the order of Debye) on-site energy from dipolar interactions can be comparable to $U^c_{||}$. As opposed to the case of contact interactions, the ratio $U^d_\perp/U^d_{||}$ depends on V_0^z/V_0. For the case $V_0^z = 2V_0$ we get $U^d_\perp/U^d_{||} \simeq 4.43$. Hund exchange is dominated by the contact interactions, $J_H \sim U^c_{||}/3$. One can tune model parameters in Eq. (3) from $\alpha \simeq 3$, $\Delta \gg 1$ (corresponding to the case of weakly polarized dipoles) to $\alpha < 2$, $\Delta < 1$ by aligning dipoles perpendicular to the zigzag plane with electric field.

[1] M. Greiner, O. Mandel, T. Esslinger, T. W. Hänsch, and I. Bloch, Nature (London) **415**, 39 (2002).
[2] M. Lewenstein, A. Sanpera, V. Ahufinger, B. Damski, A. Sen, and U. Sen, Adv. Phys. **56**, 243 (2007).
[3] T. Giamarchi, C. Rüegg, and O. Tchernyshyov, Nat. Phys. **4**, 198 (2008).
[4] I. Bloch, J. Dalibard, and W. Zwerger, Rev. Mod. Phys. **80**, 885 (2008).
[5] J. Struck, C. Ölschläger, R. Le Targat, P. Soltan-Panahi, A. Eckardt, M. Lewenstein, P. Windpassinger, and K. Sengstock, Science **333**, 996 (2011).
[6] S. Sachdev, Nat. Phys. **4**, 173 (2008).
[7] L. Balents, Nature (London) **464**, 199 (2010).
[8] S. Trotzky, Y. A. Chen, U. Schnorrberger, P. Cheinet, and I. Bloch, Phys. Rev. Lett. **105**, 265303 (2010).
[9] A. de Paz, A. Sharma, A. Chotia, E. Maréchal, J. H. Huckans, P. Pedri, L. Santos, O. Gorceix, L. Vernac, and B. Laburthe-Tolra, Phys. Rev. Lett. **111**, 185305 (2013).
[10] D. C. McKay and B. DeMarco, Rep. Prog. Phys. **74**, 054401 (2011).
[11] C. Wu, D. Bergman, L. Balents, and S. Das Sarma, Phys. Rev. Lett. **99**, 070401 (2007).
[12] X. Li, Z. Zhang, and W.V. Liu, Phys. Rev. Lett. **108**, 175302 (2012).
[13] G. Wirth, M. Ölschläger, and A. Hemmerich, Nat. Phys. **7**, 147 (2011).
[14] M. Ölschläger, T. Kock, G. Wirth, A. Ewerbeck, C. Morais Smith, and A. Hemmerich, New J. Phys. **15**, 083041 (2013).
[15] K. Aikawa, D. Akamatsu, J. Kobayashi, M. Ueda, T. Kishimoto, and S. Inouye, New J. Phys. **11**, 055035 (2009).
[16] S. Ospelkaus, K.-K. Ni, G. Quéméner, B. Neyenhuis, D. Wang, M. H. G. de Miranda, J. L. Bohn, J. Ye, and D. S. Jin, Phys. Rev. Lett. **104**, 030402 (2010).
[17] G. Sun, G. Jackeli, L. Santos, and T. Vekua, Phys. Rev. B **86**, 155159 (2012).
[18] S. Ospelkaus (private communication).
[19] S. Greschner, L. Santos, and T. Vekua, Phys. Rev. A **87**, 033609 (2013).
[20] M. J. Konstantinović, J. van den Brink, Z. V. Popovic, V. V. Moshchalkov, M. Isobe, and Y. Ueda, Phys. Rev. B **69**, 020409(R) (2004).
[21] T. Hikihara and Y. Motome, Phys. Rev. B **70**, 214404 (2004).
[22] G. Jackeli and G. Khaliullin, Phys. Rev. Lett. **103**, 067205 (2009).
[23] G. Sun, A. K. Kolezhuk, L. Santos, and T. Vekua, Phys. Rev. B **89**, 134420 (2014).
[24] F. D. M. Haldane, Phys. Lett. A **93**, 464 (1983); Phys. Rev. Lett. **50**, 1153 (1983).
[25] M. den Nijs and K. Rommelse, Phys. Rev. B **40**, 4709 (1989).
[26] H. T. Diep, *Frustrated Spin Systems* (World Scientific, Singapore, 2004).
[27] J. Villain, R. Bidaux, J. P. Carton, and R. Conte, J. Phisique **41**, 1263 (1980).
[28] A. Chubukov, Phys. Rev. Lett. **69**, 832 (1992).
[29] E. Rastelli and A. Tassi, J. Phys. C **20**, L303 (1987).
[30] C. L. Henley, Phys. Rev. Lett. **62**, 2056 (1989).
[31] J. L. Song, G. W. Semenoff, and F. Zhou, Phys. Rev. Lett. **98**, 160408 (2007).
[32] A. M. Turner, R. Barnett, E. Demler, and A. Vishwanath, Phys. Rev. Lett. **98**, 190404 (2007).
[33] G. Jackeli and D. A. Ivanov, Phys. Rev. B **76**, 132407 (2007).
[34] C. K. Majumdar and D. K. Ghosh, J. Math. Phys. **10**, 1399 (1969).
[35] S. Furukawa, M. Sato, and S. Onoda, Phys. Rev. Lett. **105**, 257205 (2010); M. Sato *et al.*, Mod. Phys. Lett. B **25**, 901 (2011); S. Furukawa, M. Sato, S. Onoda, and A. Furusaki, Phys. Rev. B **86**, 094417 (2012).
[36] S. R. White, Phys. Rev. Lett. **69**, 2863 (1992); Phys. Rev. B **48**, 10345 (1993).
[37] T. Kennedy and H. Tasaki, Phys. Rev. B **45**, 304 (1992); Commun. Math. Phys. **147**, 431 (1992).
[38] W.-L. You, Y.-W. Li, and S.-J. Gu, Phys. Rev. E **76**, 022101 (2007).
[39] L. Campos Venuti and P. Zanardi, Phys. Rev. Lett. **99**, 095701 (2007).
[40] R. Chitra, S. Pati, H. R. Krishnamurthy, D. Sen, and S. Ramasesha, Phys. Rev. B **52**, 6581 (1995).
[41] S. R. White, Phys. Rev. B **53**, 52 (1996).
[42] S. Brehmer, H. J. Mikeska, and U. Neugebauer, J. Phys.: Condens. Matter **8**, 7161 (1996).
[43] C. Castellani, C. R. Natoli, and J. Ranninger, Phys. Rev. B **18**, 4945 (1978).
[44] T. Sowiński, M. Łącki, O. Dutta, J. Pietraszewicz, P. Sierant, M. Gajda, J. Zakrzewski, and M. Lewenstein, Phys. Rev. Lett. **111**, 215302 (2013).
[45] K. Góral, K. Rzążewski, and T. Pfau, Phys. Rev. A **61**, 051601(R) (2000).
[46] C. Trefzger, C. Menotti, B. Capogrosso-Sansone, and M. Lewenstein, J. Phys. B: At. Mol. Opt. Phys. **44**, 193001 (2011).